To be published in Rough Surface Scattering and Contamination, P.-T. Chen, Z.-H. Gu, and A. A. Maradudin, Editors., Proc. SPIE 3784 (1999).

Polarization of light scattered by spheres on a dielectric film

Lipiin Sung,[a,b] George W. Mulholland,[a] and Thomas A. Germer[a]

[a]*National Institute of Standards and Technology, Gaithersburg, MD 20899*
[b]*University of Maryland, College Park, MD 20742*

ABSTRACT

Bidirectional ellipsometric measurements were conducted on a model system containing spherical particles on silicon surfaces coated with dielectric polymer films. The principal angle of polarization, $\eta^{(\mathrm{p})}$, and the degree of linear polarization, $P_{\mathrm{L}}^{(\mathrm{p})}$, of the light scattered into directions out of the plane of incidence were measured using p-polarized, 532 nm light. Results are presented and compared to those from particles on a bare silicon substrate. Spheres of diameter 181 nm and 217 nm and film thicknesses ranging from 55 nm to 140 nm were used to test two theoretical models for light scattering: a Mie-surface double-interaction approximation and a finite-element time-domain implementation of Maxwell's equations. The measurements and the modeling demonstrate the application of bidirectional ellipsometry for characterizing the sizes of particulate contaminates on surfaces.

Keywords: dielectric films, ellipsometry, polystyrene latex spheres, polarimetry, scattered light.

1. INTRODUCTION

Developing and testing theories and models necessary to interpret the light scattering behavior of a wide variety of surfaces is of great interest to the microelectronics, optics, and data storage industries. Transferring the knowledge base acquired from the study of well-characterized model systems to that necessary for characterization of real-world materials may be difficult. It is our goal to develop methodologies to address this transition by specifically investigating model systems designed to simulate light scattering from various sources, such as surface microroughness, particulate contamination, and subsurface defects. Experimentally, model systems consisting of spherical particles on a single silicon surface, roughness in a dielectric film on a silicon surface, and spherical particles above a dielectric film on a silicon surface are designed to simulate the types of scatter sources found on single surfaces and near dielectric films.

Recent studies[1–4] have shown that the polarization of scattered light can be used to characterize and distinguish amongst various types of features near surfaces, such as surface topography, particulate contamination, and defects. Moreover, a study on a model system, containing polystyrene latex (PSL) spheres on a silicon surface, demonstrated that the polarization of light scattered from particles on a surface can be used to determine the size of those particles.[4] Bidirectional ellipsometric (BE) measurements, whereby the principal angle of polarization, $\eta^{(\mathrm{p})}$, and the degree of linear polarization, $P_{\mathrm{L}}^{(\mathrm{p})}$, of light scattered into directions out of the plane of incidence are measured for p-polarized incident light, were carried out on this model system and compared to theoretical models. The theoretical calculations, based upon the discrete dipole approximation (DDA),[5] predicted the overall trends of the angular dependence of the measured BE parameters as functions of the sphere diameter. Furthermore, comparison of the DDA results with those using simpler approximations,[1,6–9] indicated that the dominant factor determining the scattered light polarization is the mean distance of a particle from the surface. This finding suggests that the results can be applied to non-spherical particles and particles of unknown optical properties.

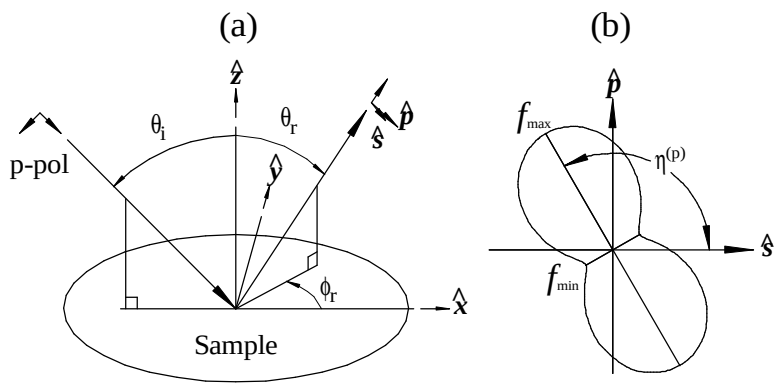

Figure 1 (a) The sample coordinate system used in this paper; and (b) a schematic of the intensity f measured by a rotating linear-polarization-sensitive detector, defining the bidirectional ellipsometry parameters, $\eta^{(\mathrm{p})}$ and $P_{\mathrm{L}}^{(\mathrm{p})} = (f_{\max} - f_{\min})/(f_{\max} + f_{\min})$.

In this paper, we have extended our study to spheres deposited upon a dielectric layer on silicon. Experimental results for systems consisting of various sphere sizes and film thickesses will be presented and compared to theoretical light scattering calculations. Theoretical calculations, based on a Mie-surface double-interaction (MSDI) model and the finite-element time-domain (FETD) approximation, describe the angular dependence of the BE data qualitatively, and predict the general trend of the BE data as functions of film thickness. As expected, the presence of the dielectric layer has a pronounced effect on the BE parameters for identically-sized spheres.

In Sec. 2, we describe the sample preparation and experimental procedure employed for these measurements. In Sec. 3, the MSDI model and the FETD calculations are described. In Sec. 4, the experimental and theoretical results are presented and discussed. Finally, the results are summarized in Sec. 5.

2. EXPERIMENT

2.1 Bidirectional Ellipsometry

Figure 1(a) shows the optical geometry used in this study. Laser light of wavelength $\lambda = 532$ nm and p-polarization is incident onto a sample at an angle θ_{i}. The light scattered into a solid angle $\Omega \approx 10^{-4}$ sr centered on a polar angle θ_{r} and azimuthal (out-of-plane) angle ϕ_{r} is collected by a rotating linear-polarization-sensitive detector. Figure 1(b) illustrates schematically a typical scattering signal one obtains as the detector is rotated. Bidirectional ellipsometric (BE) measurements are presented in terms of the principal angle of polarization, $\eta^{(\mathrm{p})}$, and the degree of linear polarization, $P_{\mathrm{L}}^{(\mathrm{p})}$, as functions of ϕ_{r} for fixed θ_{i} and θ_{r}. In all of the measurements presented in this paper, $\theta_{\mathrm{i}} = \theta_{\mathrm{r}} = 45°$. Out-of-plane BE measurements with p-polarized incident light have been found to optimize the distinction amongst different scattering mechanisms.[2–4,10–12]

2.2 Sample Preparation

The model system used in this study consists of polystyrene latex (PSL) spheres on a silicon wafer precoated with a polystyrene (PS) film (see Fig. 2). Films with thicknesses $t = 55$ nm to 140 nm were prepared using the spin-cast technique. For low polymer concentrations and fixed molar mass of polystyrene, the film thickness is found to be roughly proportional to $c_{\mathrm{p}}^{1/3}\omega^{-1/2}$, where c_{p} is the concentration of the PS (molar mass of 22 000 g/mol) in toluene, and ω is the spin-cast angular speed.[13] Before spin-casting, the solutions were filtered through a 0.4 μm pore-size filter to remove impurities. As cast, all films appeared homogeneous and uniform under an optical microscope. The actual film thicknesses were determined by single-wavelength specular rotating-analyzer ellipsometric measurements at various incident angles.[14] We used literature values for the complex indices of

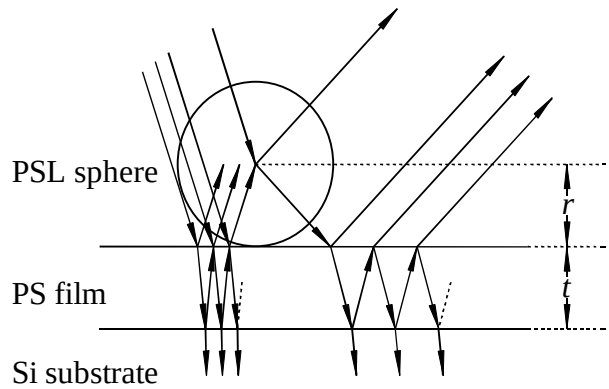

Figure 2 Schematic diagram illustrating the Mie-surface double-interaction (MSDI) model for light scattering from a sphere on a dielectric layer, where r is the radius of the PSL sphere, and t is the PS film thickness.

refraction of silicon ($n_{\mathrm{Si}} = 4.15 + 0.05i$), PS ($n_{\mathrm{PS}} = 1.59$), and PSL ($n_{\mathrm{PSL}} = 1.59$) at $\lambda = 532$ nm.[15] The film thicknesses determined using ellipsometry are consistent with those obtained from x-ray reflectivity. The uncertainty in the film thickness is about 2 nm (at 95 % confidence level), estimated from statistical data analysis from multiple measurements and comparison with results obtained from x-ray reflectivity.

A low-pressure impactor connected to a particle generation/classification system was used to deposit monodisperse PSL spheres having diameters 181 nm and 217 nm. Details of the deposition method and the particle size analysis are described elsewhere.[16–18] Using optical microsopy, we measured the surface densities of PSL spheres to be about 30 000 mm^{-2} in the illuminated sample regions, and found that less than 2 % of the particles were doublets (two touching spheres). The overall scattering intensity from the samples with PSL spheres is about two orders of magnitude stronger than the light scattered from the samples with only PS films, so that the light scattering from the roughness of the PS film in the sphere/film/Si system should be negligible. The particle densities used in this study were low enough that direct particle-particle interactions can be ignored. However, they were high enough that structure factors, which are related to particle-particle correlation functions and are affected by roughness, could not be assumed to be constant. Therefore, the results of intensity measurement will not be presented in this paper.

3.THEORY

We will use two theoretical models to compare with the experimental data. The first, the MSDI model, illustrated in Fig. 2, is computationally efficient and conceptually relatively simple.[9] A sphere is assumed to be illuminated by two plane waves, one directly from the source, and the second reflected from the film. A phase and amplitude difference between these two waves results from the path length difference and the Fresnel reflection coefficients of the film. The diffraction from the sphere, given by the exact Mie solution for a sphere in free space,[7,8] dictates the angular dependence of the amplitude and polarization of the scattered light. The total scattered light is a result of interference between light scattered directly to the detector and that scattered through reflection in the film. Although shadow functions are commonly employed in this model,[9] we believe that their use is inappropriate for small transparent particles; they result in polarizations significantly different from the data, and they are not included in our analysis.

The MSDI model was found to give excellent agreement with experimental data for $\eta^{(\mathrm{p})}$ at small and medium scattering angles for dielectric spheres on bare silicon.[4] However, it does not include the near-field interaction between the sphere and its image in the surface, which has a noticeable effect on $P_{\mathrm{L}}^{(\mathrm{p})}$ at all scattering angles and

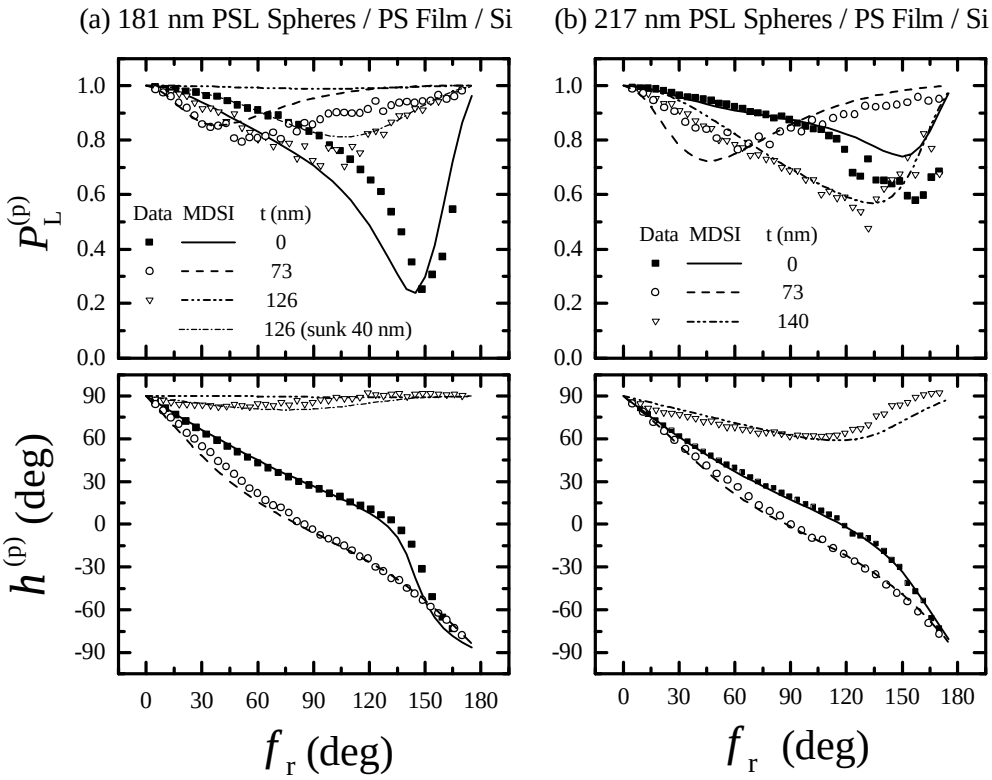

Figure 3 (a) BE parameters for 181 nm PSL spheres on bare silicon and silicon coated with PS films of two film thicknesses. The curves represent the theoretical predictions using the MSDI model. (b) Same as (a), except for 217 nm PSL spheres. The measurement uncertainties are dominated by statistical sources and are typically smaller than the size of the symbols used in the graphs or the statistical spread in the data from point to point, whichever is larger.

on $\eta^{(p)}$ at large scattering angles. For that reason, and to evaluate the accuracy of the MSDI model, we have also performed finite-element time-domain calculations using the commercially-available EMFLEX program.[19,20] The code solves Maxwell's equations on a finite-element grid in the time domain, beginning with field conditions given by the exact solution without the particle, and ending after steady state is reached. The three-dimensional grid is chosen so that the shortest length of each rectangular element is $\lambda/20$ or smaller in each material. The grid extends a distance λ above the particle, λ/n_{Si} into the silicon substrate, and 2.5λ in each lateral direction. Symmetry boundary conditions were used for the plane of incidence. Illumination boundary conditions were used for all the other edges of the model. To obtain far-field amplitudes, a vector Kirchhoff integral is performed, using a surface of integration chosen to be large enough that the fields are negligible at its edges. The electric field in the direction parallel to the direction of propagation was less than 0.01 of the total field. Due to limitations of EMFLEX, the index of refraction of the silicon was assumed to be real, $n_{\mathrm{Si}} = 4.15$. In all calculations, it is assumed that the spheres are isolated. Unlike the MSDI calculations, which are simple and computationally efficient, taking less than a second on a desktop computer, the FETD calculations are complex and time consuming, taking hours on a high-end workstation.

TABLE 1 The extracted values of the initial slope $-d\eta^{(\mathrm{p})}/d\phi_{\mathrm{r}}$ obtained from the experimental data and theoretical models (MSDI and FETD). The uncertainties ($\pm 2\sigma$) were evaluated by a standard statistical data analysis from the linear regression of data in the low ϕ_{r} region.

D (nm)	t (nm)	Experiment	MSDI	FETD
181	0	0.79 ± 0.04	0.81	0.94
181	55	1.26 ± 0.15	1.60	1.49
181	73	1.13 ± 0.05	1.41	1.27
181	126	0.27 ± 0.09	0.00	0.08
217	0	0.95 ± 0.03	0.98	1.11
217	55	1.28 ± 0.04	1.50	1.34
217	73	1.00 ± 0.12	1.06	0.98
217	140	0.44 ± 0.26	0.33	0.43

4. RESULTS AND DISCUSSION

Figure 3 shows the measured BE parameters as functions of ϕ_{r} for different sphere diameters on different film thicknesses and on a bare wafer. The curves represent the predictions of the MSDI model and will be discussed later in the text. The experimental results indicate that BE parameters for a given sphere size depend strongly on the film thickness and can be distinguished from those for the same size sphere on a bare wafer. This finding is in agreement with our understanding that the particle effectively samples the local field a distance from the surface given by the radius of the particle, and radiates from that same position. The presence of the dielectric layer affects the amplitudes and phases of the reflection coefficients of the surface, and thus affects the local field at the particle. Comparison of the results in Fig. 3 for the two sphere sizes suggests that for some film thicknesses (e.g. $t \sim 130$ nm), the two sphere sizes can be differentiated, while for others (e.g. $t = 73$ nm), they cannot.

The previous results for dielectric spheres on bare silicon demonstrated that the sizes of spheres can be estimated by the ϕ_{r}-dependence of $\eta^{(\mathrm{p})}$ for small ϕ_{r}.[4] One might expect a similar behavior for the spheres on dielectric films. Table 1 shows the extracted values of the initial slope $-d\eta^{(\mathrm{p})}/d\phi_{\mathrm{r}}$ obtained from the experimental results, and from the MSDI and FETD calculations. Unlike the results for a bare silicon wafer, the two sizes cannot always be distinguished by this method.

Before comparing the experimental data to the theoretical calculations, it is worth comparing the MSDI and FETD calculations in order to assess their validity. Figure 4 shows a comparison between the BE parameters and the differential scattering cross sections calculated by the two methods. One can see that these two methods are in fairly good agreement with each other. The fact that these two very different approaches give similar results suggests that neither is far from an exact solution. It is known that the MSDI model ignores near-field and shadow effects, and that the FETD calculations have constraints due to the finite size of the simulation volume. Small wiggles in the FETD curves (especially for $P_{\mathrm{L}}^{(\mathrm{p})}$), for example, can be traced to imperfect illumination boundary conditions. The good agreement between the theoretical methods, and their disparate calculation times, suggests that the MSDI model is adequate for predicting inspection instrument performance with these types of defects.

Figure 3 shows the predictions of the MSDI model with the data. The overall agreement is very good, although some improvement could be made. The differences may be due to inaccuracies in the model—compare the level of agreement between the two models in Fig. 4 with the level of agreement between the MSDI model and the data in Fig. 3. Possible experimental errors may result from interactions between particles, existence of non-spherical particles on the surface, or from interference with other scattering sources such as subsurface defects or microroughness. Random sources of scatter, such as these, are expected to depolarize the light. In addition to the experimental data, Table 1 shows calculated values of $-d\eta^{(\mathrm{p})}/d\phi_{\mathrm{r}}$ using the two models. The

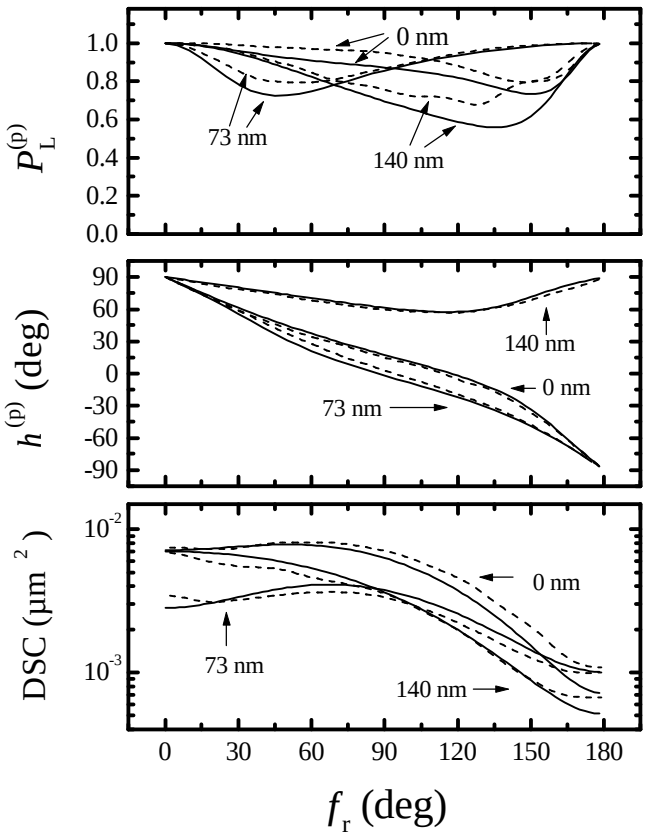

Figure 4 Comparison of theoretical bidirectional ellipsometry parameters, $\eta^{(p)}$ and $P_L^{(p)}$, and the differential scattering cross section, DSC, from the MSDI model with those from the finite-element time-domain (FETD) calculations for a 217 nm sphere on a PS dielectric layer with different film thicknesses. The solid curves represent the MSDI model while the dashed curves represent the FETD calculations.

FETD calculations show a slightly better agreement with data than the MSDI model, especially for 217 nm spheres.

It is interesting to note that improvements can be made in the comparison between the experiment and the theory for 181 nm PSL spheres on a 126 nm film, if one assumes that the spheres are partially embedded in the film. One of the theoretical curves in Fig. 3(a) was calculated assuming that the sphere was sunken into the film a distance of 40 nm. The agreement improves substantially for both $\eta^{(p)}$ and $P_L^{(p)}$. Similar results were found for a 181 nm PSL spheres on a 55 nm film. Investigations using atomic force microscopy (AFM) are ongoing to clarify this issue. In addition, experiments on samples having a more robust film material, such as silicon dioxide, will be carried out.

Figure 5 shows the slope $-d\eta^{(p)}/d\phi_r$, evaluated at $\phi_r = 0$, using the MSDI model for $\theta_i = \theta_r = 45°$ and $\lambda = 532$ nm for different film thicknesses and sphere diameters. It can be seen that two extrema exist for a bare wafer: one is very near to zero diameter and another extremum exists around $D = 250$ nm. The presence of the thin film causes this extremum to move towards smaller sphere diameter and introduces new ones for larger sphere diameter. When the sphere diameter is near one of these extrema, it is difficult to accurately estimate the size of the sphere using polarization information alone. This effect can be seen in Table 1, where it is difficult to

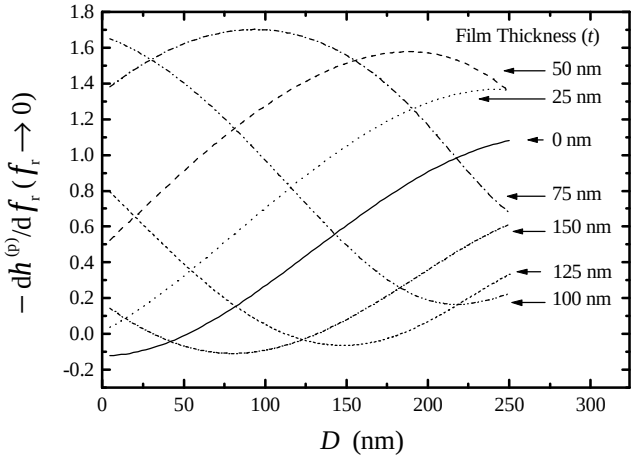

Figure 5 Curves of $-d\eta^{(\mathrm{p})}/d\phi_{\mathrm{r}}$, evaluated at $\phi_{\mathrm{r}} = 0$, using the Mie-surface double interaction (MSDI) model, as functions of sphere diameter, for different film thicknesses. The incident and scattering angles were $\theta_{\mathrm{i}} = \theta_{\mathrm{r}} = 45°$, and the wavelength $\lambda = 532$ nm.

distinguish between 181 nm and 217 nm spheres on the 55 nm and 73 nm films. The locations of these extrema depend upon θ_{i}, θ_{r}, and λ, so that this lack of specificity can be changed by using different scattering geometries or wavelengths.

4. SUMMARY

The polarization of light scattered by model systems containing PSL spheres on silicon wafers coated with PS films was measured, and the results were compared to predictions based on the MSDI model and FETD calculations. We demonstrate that the polarization of light scattered from spheres on different film thicknesses can be distinguished from that scattered from spheres on bare silicon, and can be used to estimate the sizes of particulate contaminates on surfaces containing dielectric films. The simple and computationally efficient MSDI model describes experimental results well and can be used to predict the general trend of the angular dependence of the BE parameters in the presence of a dielectric layer.

ACKNOWLEDGMENTS

The authors would like to thank Mr. Marco Fernandez for assisting in the particle depositions.

REFERENCES

[1] T. A. Germer, "Angular dependence and polarization of out-of-plane optical scattering from particulate contamination, subsurface defects, and surface microroughness," Appl. Opt. **36**, 8798 (1997).

[2] T. A. Germer and C. C. Asmail, "Polarization of light scattered by microrough surfaces and subsurface defects," J. Opt. Soc. Am. A**16**, 1326 (1999).

[3] T. A. Germer, C. C. Asmail, and B. W. Scheer, "Polarization of out-of-plane scattering from microrough silicon," Opt. Lett. **22**, 1284 (1997).

[4] L. Sung, G. W. Mulholland, and T. A. Germer, "Polarized light scattering measurements of dielectric spheres on a silicon surface," Opt. Lett., **24**, 866 (1999).

[5] R. Schmehl, B. M. Nebeker, and E. D. Hirleman, "Discrete-dipole approximation for scattering by features on surfaces by means of a two-dimensional fast Fourier transform technique," J. Opt. Soc. Am. A**14**, 3026 (1997).

[6] G. Videen, W. L. Wolfe and W. S. Bickel, "Light scattering Mueller matrix for a surface contaminated by a single particle in the Raleigh limit," Opt. Eng. **31**, 341 (1992).

[7] H. C. van de Hulst, *Light Scattering by Small Particles* (Dover, New York, 1981).

[8] F.C. Bohren and D. R. Huffman, *Absorption and Scattering of Light by Small Particles* (Wiley, New York, 1983).

[9] K. B. Nahm and W. L. Wolfe, "Light-scattering models for spheres on a conducting plane: comparison with experiment," Appl. Opt. **26**, 2995 (1987).

[10] T. A. Germer and C. C. Asmail, "A goniometric optical scatter instrument for bidirectional reflectance distribution function measurements with out-of-plane and polarimetry capabilities," in *Scattering and Surface Roughness*, Z.-H. Gu, and A. A. Maradudin, eds., Proc. SPIE **3141**, 220 (1997).

[11] T. A. Germer and C. C. Asmail, "Goniometric optical scatter instrument for out-of-plane ellipsometry measurements," Rev. Sci. Instrum., in press (1999).

[13] D. B. Hall, P. Underhill, and J. M. Torkelson, "Spin coating of thin and ultrathin polymer films," Polym. Eng. and Sci. **38**, 2039, (1998).

[14] R.M.A. Azzam and N.M. Bashara, *Ellipsometry and Polarized Light* (Elsevier, Neitherland, 1987).

[15] J. Brandrup and E. H. Immergut, *Polymer Handbook* (Wiley, New York, 1989).

[16] P. D. Kinney, D. Y. H. Pui, G. W. Mulholland, and N. P. Bryner, "Use of the electrostatic classification method to size 0.1 μm SRM particles—a feasibility study," J. Res. Natl. Inst. Stand. Technol. **96**, 147 (1991).

[17] S. V. Hering, S. K. Friedlander, J. J. Collins, and L. W. Richards, "Design and evaluation of a new low-pressure impactor. 2," Env. Sci. Technol. **13**, 184 (1979).

[18] G. W. Mulholland, N. P. Bryner, and C. Croarkin, "Measurement of 100 nm NIST SRM 1963 by differential mobility analysis," J. Aersol Sci. and Technol., in press.

[19] Certain commercial software are identified in this paper in order to specify the procedure adequately. Such identification is not intended to imply recommendation or endorsement by the National Institute of Standards and Technology, nor is it intended to imply that the software identified is necessarily the best available for the purpose.

[20] EMFLEX is available from Weidlinger Associates, Inc., Los Altos, CA.